

Pressure-dependent magnetization and magnetoresistivity studies on the tetragonal FeS (mackinawite): revealing its intrinsic metallic character

S. J. Denholme,¹ H. Okazaki,¹ S. Demura,¹ K. Deguchi,¹ M. Fujioka,¹ T. Yamaguchi,¹ H. Takeya,¹ M. ElMassalami,² H. Fujiwara,³ T. Wakita,⁴ T. Yokoya,⁴ and Y. Takano¹

¹*National Institute for Materials Science, 1-2-1, Sengen, Tsukuba, 305-0047, Japan*

²*Instituto de Física, Universidade Federal do Rio de Janeiro, Caixa Postal 68528, 21941-972 Rio de Janeiro RJ, Brazil*

³*Research laboratory for surface science, Okayama University, Okayama,*

⁴*Research laboratory for surface science, Okayama University, Okayama, 700-8530, Japan*

The transport and magnetic properties of the tetragonal $\text{Fe}_{1+\delta}\text{S}$ were investigated using magnetoresistivity and magnetization within $2 \leq T \leq 300$ K, $H \leq 70$ kOe and $P \leq 3.0$ GPa. In addition, room-temperature X-ray diffraction and photoelectron spectroscopy were also applied. In contrast to previously reported nonmetallic character, $\text{Fe}_{1+\delta}\text{S}$ is intrinsically metallic but due to a presence of a weak localization such metallic character is not exhibited below room temperature. An applied pressure reduces strongly this additional resistive contribution and as such enhances the temperature range of the metallic character which, for ~ 3 GPa, is evident down to 75 K. The absence of superconductivity as well as the mechanism behind the weak localization will be discussed.

PACS numbers: 74.70.Xa, 72.15.Rn, 78.40.Pg

I. INTRODUCTION

Although the isomorphous Fe-based chalcogenides $\text{Fe}_{1+\delta}\text{X}$ ($\text{X} = \text{Te}, \text{Se}, \text{S}$) crystallize into the room-temperature tetragonal $P4/nmm$ structure, however (as far as the *low-temperature* structural, magnetic, and electronic properties are concerned) their phase diagrams¹⁻⁶ are distinctly different: $\text{Fe}_{1+\delta}\text{Se}$ is an orthorhombic nonmagnetic superconductor; $\text{Fe}_{1+\delta}\text{Te}$ is a monoclinic antiferromagnetic metal while $\text{Fe}_{1+\delta}\text{S}$ is a tetragonal nonmagnetic and nonconducting compound⁷⁻⁹ though, in sharp contrast, most theoretical work suggests metallic character.¹⁰⁻¹² Further distinction among these $\text{Fe}_{1+\delta}\text{X}$ is evident in the response of their individual states to applied pressure, doping, intercalation, or a magnetic field. Most striking are the differences among the superconducting phase diagrams of their solid solutions, e.g. $\text{Fe}_{1+\delta}(\text{Te}_{1-x}\text{X}_x)$ ($\text{X} = \text{Se}, \text{S}$):^{1,2} substitution leads to a gradual suppression of magnetism and to an eventual surge of superconductivity; on the other hand, for $\text{Fe}_{1+\delta}(\text{Se}_{1-x}\text{S}_x)$, substitution leads to a slight enhancement in T_c up to $x=0.2$ but on further substitution the superconducting transition is monotonically suppressed.

It is remarkable that in spite of such a distinction between the electronic states of these $\text{Fe}_{1+\delta}\text{X}$ compounds, theoretical studies¹⁰⁻¹² predicted a metallic normal-state: while this metallicity is established for *low-temperature* phases of $\text{Fe}_{1+\delta}\text{Te}$ and $\text{Fe}_{1+\delta}\text{Se}$, experimentally $\text{Fe}_{1+\delta}\text{S}$ was reported to manifest an absence of metallic conductivity.⁷ As that the question of the electronic character of $\text{Fe}_{1+\delta}\text{S}$ is of a fundamental importance to the general understanding of the normal and superconducting phase diagrams of these Fe-based chalcogenides, this work addresses the electronic properties of $\text{Fe}_{1+\delta}\text{S}$ using X-ray diffraction, spectroscopic (ultra violet photoelectron spectroscopy, UPS), and thermodynamic (mag-

netoresistivity and magnetization over a wide range of temperature T , pressure P , and magnetic field H) techniques

Based on the stoichiometry of the iron monosulfides FeS, there are, in general, three classes:⁸ (i) this $\text{Fe}_{1+\delta}\text{S}$ system (mackinawite) which, just as for the other isomorphous $\text{Fe}_{1+\delta}\text{X}$, manifests an excess of Fe and crystallizes in the layered anti-PbO type structure;¹³ an application of 3.3 GPa at room temperature transforms its tetragonal phase into an orthorhombic structure.¹⁴ (ii) the near-stoichiometric and hexagonal antiferromagnetic FeS (troilite),^{15,16} and (iii) the hexagonal Fe-deficient ferromagnetic $\text{Fe}_{1-\delta}\text{S}$ ($x \leq 0.2$) which crystallizes in the nickel arsenide form (pyrrhotite).¹⁷ The structural and physical properties of both FeS and $\text{Fe}_{1-\delta}\text{S}$ have been extensively investigated;^{17,18} in contrast, $\text{Fe}_{1+\delta}\text{S}$ has been relatively unexplored except for some structural and mineralogical studies:¹⁹⁻²¹ neutron diffraction and Mössbauer analysis indicated nonmagnetic character;⁷ this contradicts an analysis done by photoelectron spectroscopy (PES)¹² which suggested, instead, a single-stripe antiferromagnetic ground state.

Electronic structure calculations^{10-12,22} on $\text{Fe}_{1+\delta}\text{S}$ indicated a significant Fe 3d orbital delocalization (primarily due to the basal-plane, intralayer Fe-Fe interactions), a dominant 3d contribution to the density of states (DOS, $N(E_F)$) at the Fermi level, E_F , and a weaker hybridization between the Fe and S.¹⁰⁻¹² As mentioned above such a predicted metallic character is in disagreement with the experimentally observed nonmetallicity. In this work, we show that $\text{Fe}_{1+\delta}\text{S}$ is indeed metallic just as theoretically predicted; the reported nonmetallicity^{7,23} will be shown to be due to a localization of charge carriers. It is recalled that such a discrepancy between experiment and theory had already been reported in other transition metal sulfides:²⁴ e.g., troilite is a p-type semiconductor with a band gap of 0.04 eV;¹⁶ yet band structure

calculations have placed E_F within the d - p hybridized bands.²⁵ Similarly, a PES study on pyrrhotite reported a 25-30% narrower Fe $3d$ DOS band-width than the theoretical prediction.²⁶

II. EXPERIMENTAL

Mackinawite was synthesized using the method reported by Lennie *et al.*²⁰ Powder X-ray diffractograms on a conventional Cu $K\alpha$ diffractometer indicated a single phase $P4/nmm$ structure with $a=3.675(2)$ Å, $c=5.035(6)$ Å. Based on an energy dispersive X-ray analysis, the actual stoichiometry was found to be Fe:S=0.52:0.48 giving $\text{Fe}_{1.08}\text{S}$ which is in agreement with the reported ranges.^{20,27}

It is well-known that the tetragonal $\text{Fe}_{1+\delta}\text{S}$ is chemically unstable against a variation in P , T and aging:²⁸ aging at room temperature would slowly transform it into an amorphous product plus the semi-metallic cubic Fe_3S_4 (greigite). During this study, it became evident that (i) such a conversion can be temporarily inhibited if the sample is stored at cooler temperatures e.g. below 5 C°; (ii) this tetragonal $\text{Fe}_{1+\delta}\text{S}$, when subjected to a higher pressure, would start to convert into an amorphous product, reminiscent of the amorphization in $\text{Fe}_{1+\delta}\text{Se}$ and $\text{FeSe}_{0.5}\text{Te}_{0.5}$,²⁹ plus the semiconducting hexagonal $\text{Fe}_{1-\delta}\text{S}$ (troilite). Accordingly, such a phase instability requires that extra care should be exercised during (as well as before and after) the measurements so as to ensure that all results had been obtained on the very same tetragonal phase: otherwise most of the results (in particular the resistivity) are irreproducible. With this in mind, the following measurements and their analysis were carried out.

Resistivity, ρ , was measured using a standard four-inline method on cold-pressed pellets (care was undertaken to ensure that the grain boundary influence was minimized - see below). For $\rho(P)$, hydrostatic pressures, up to 3.0 GPa, were generated by a BeCu/NiCrAl clamped piston-cylinder cell using Fluorinert as a P -transmitting fluid while Pb as a manometer. Similarly, P -dependent magnetizations were measured using a hydrostatic pressure cell (up to 1 GPa). Daphne oil was used as a P -transmitting fluid while Sn as a manometer.

UPS was measured at a base pressure of 2.0×10^{-8} Pa and at a temperature of 300K with He I (21.2 eV), He II (40.8eV) and Xe I (8.44 eV) resonance lines. So as to obtain a fresh surface, samples were cut within an ultra-high vacuum chamber. The Fermi energy was referenced to that of an Au film which was measured frequently during the experiments.

III. RESULTS

Fig. 1(a) illustrates $\rho(T, H=0, P=0.1 \text{ MPa})$ of $\text{Fe}_{1.08}\text{S}$.^{7,23} It is remarkable that $\rho(2 \leq T \leq 300 \text{ K}) \sim \text{m}\Omega\text{-cm}$

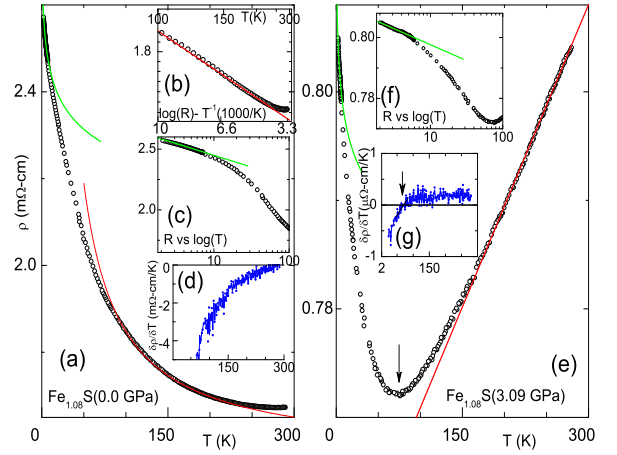


FIG. 1. Typical resistivity curves of $\text{Fe}_{1.08}\text{S}$ (a-d) under ambient-pressure while (e-g) are under an applied pressure of 3.09 GPa. (a and e) isobaric ρ vs T curves. (b) ρ vs T curve in a log-reciprocal plot emphasizing the activated process; the solid line is a fit to Eq.1. (c and f) ρ vs T curves in a linear-log plot emphasizing the weak localization behavior; the solid lines is a fit to Eq. 2. (d and g) $\frac{\partial \rho}{\partial T}$ vs T curve: a negative (positive) value represents nonmetallic- (metallic-) like behavior. The crossover point is denoted as T_L . The obtained T_L , $\frac{\partial \rho}{\partial T}$, Δ , S parameters are collected in Fig. 2.

cm suggesting that this (monotonic but non-sharp) low- T rise is not due to a conventional metal-insulator transition; most probably, it is a manifestation of localization of charge carriers³⁰⁻³² (see below). Following the analysis of Ref. 33, it is taken that the resistivity is intrinsically metallic, any nonmetallicity is attributed to this localization. Fig. 1(d) reveals such nonmetallic character as a negative $\frac{\partial \rho}{\partial T}$. Moreover, as $T \rightarrow 300\text{K}$, $\frac{\partial \rho}{\partial T} \rightarrow 0$ at $\sim 300\text{K}$: assuming a stable tetragonal phase (see Experimental), the event $\frac{\partial \rho}{\partial T}=0$ is taken as a crossover from a nonmetallic state into a metallic one. A closer look at the evolution of $\rho(T < 300 \text{ K})$ suggests that there are at least two types of localization-induced behavior.³³ The first appears to be a thermally-assisted behavior:³⁴

$$\rho(100 < T < 300\text{K}) = \rho_0^A \exp(\Delta/T). \quad (1)$$

Such a thermally activated ($\Delta \sim 20 \text{ K}$) process [see Fig. 1(b)] is assumed to be due to a hopping of carriers from one localized state into an itinerant state that is separated by an effective $\Delta = |E - E_c|$ where E_c is the mobility edge³⁴ and should not be confused with the conventional semiconducting behavior. A manifestation of an activated behavior below a crossover/transition was already observed in RNiO_3 .³⁵ The second process looks like a weak-localization process which is often encountered in the low- T phase of a disordered metal.³⁰⁻³² In chalcogenides,³³ the disorder is attributed to the nonperiodic scattering potentials (see below). Then their $\rho(T)$ should follow³⁰⁻³²

$$\rho(T < 20\text{K}) = \rho_o^L [1 + S \ln(T_o/T)] \quad (2)$$

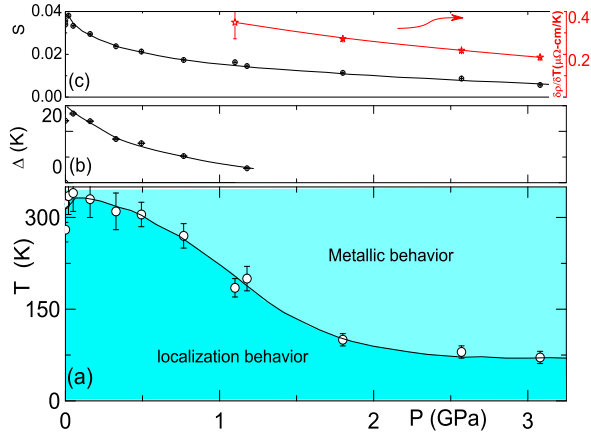


FIG. 2. The baric evolution of (a) T_L of $\text{Fe}_{1.08}\text{S}$ (a measure of localization strength which is emphasized below $T_L(P)$ curve), (b) Δ (the activation energy in Eq. 1) (c) *left ordinate*: S (as a measure of strength of the localization process below 20 K, see Eq. 2); *right ordinate*: $\frac{\partial \rho}{\partial T}$ within $T_L < T < 300$ K (a measure of the thermal evolution of the metallic resistivity).

where S is a measure of the scattering process while T_o and ρ_o^L are any measured pair [Fig. 1(c)]. Such a log-in- T character was already reported for other chalcogenides.^{4,33,36} Presently it is not evident why this process is not proceeded by a metallic-like state as observed in, e.g., Ref.[33].

An application of pressure leads to pronounced effects: e.g. (i) on comparing $\rho(T)$ of panels (a) and (e) of Fig. 1, one notices a reduction in the overall resistivity, and (ii) the crossover point signalled by $\frac{\partial \rho}{\partial T}=0$, denoted as $T_L(P)$, moves to well below 300K: the metallicity is pressure-enhanced to a wide range of temperature.³⁵

Just as for the ambient-pressure case, $\rho(T < T_L, P)$ of Fig. 1(e) was analyzed in terms of the above mentioned two processes. The baric evolution of the fit parameters are shown in Fig. 2; P reduces all scattering processes: a monotonic decrease of (i) $\frac{\partial \rho}{\partial T}$ within the metallic state, (ii) Δ within the activated region, and (iii) S below 20 K. All these influences lead to a strong reduction of $T_L(P < 2\text{GPa})$. Above 2 GPa, $T_L(P)$ is weakly but monotonically decreasing till $T_L(P = 3.1\text{GPa}) \sim 75$ K; such a thermal evolution is also manifested for each of the parameters shown in Fig. 2(b-c).

Fig.2(a) identifies unambiguously the metallic state as being an intrinsic high- T property of $\text{Fe}_{1+\delta}\text{S}$: this provides a direct confirmation of the theoretical predictions. Evidently, without the clarification provided by the high- P or high- T $\rho(T, P)$ curves, the activated rise in $\rho(T < 300$ K) as T is lowered would be mistakenly taken as indicative of intrinsic nonmetallic conductivity.^{7-9,23}

Various possible mechanisms can give rise to the pressure influence on each of the $\frac{\partial \rho}{\partial T}$, Δ , S parameters (Fig. 2); two of which are (i) the cold-pressed pelletizing process brings together the already metallic grains; as such an application of further pressure (during the $\rho(T, P)$

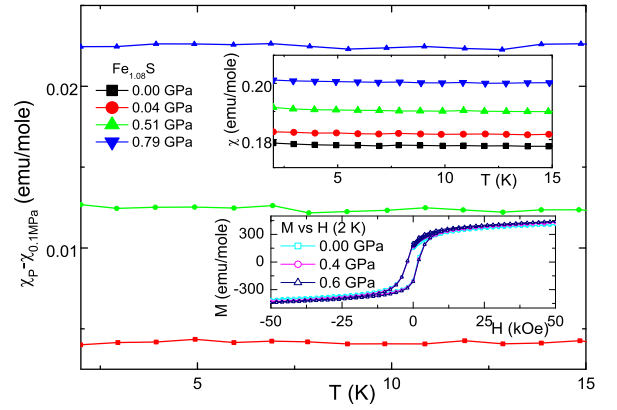


FIG. 3. The excess, pressure-dependent molar susceptibility of $\text{Fe}_{1.08}\text{S}$. The ambient pressure $\chi(T, P=0.0\text{ GPa})$ curve (upper inset) is similar to that of Sines *et al.*³⁷ As the total contribution includes those of weak magnetic impurities and the cell body and as that these contributions are not influenced by P (see the two insets), then, for clarity, these contributions are subtracted out by plotting, in the main frame, $\Delta\chi(T, P) = \chi(T, P) - \chi(T, 0.0\text{ GPa})$.

measurement) would lead to a further enhancement of the grain connectivity. (ii) The influence of the pressure is intrinsic both on the involved scattering processes as well as on the electronic structure of $\text{Fe}_{1+\delta}\text{S}$. To differentiate between which of these is the most plausible mechanism, we carried out a magnetization measurements. Based on the above, $\text{Fe}_{1+\delta}\text{S}$ is expected to be a nonmagnetic metal, thus its $\chi(T)$ should be constant-in- T , Pauli-like and proportional to $N(E_F)$. If the observed P -induced effects are due to grains connectivity then $\chi(T)$ should not be influenced. If, otherwise, P influences its nonpolarized electronic structure, then its $\chi(T)$ should also be modified. Indeed Fig. 3 indicates a P -induced enhancement of χ and as such an enhancement of $N(E_F)$: this is in an excellent agreement with the P -induced enhancement of the conductivity observed in Fig. 1.

The general features of Figs. 1-2 can also be interpreted in terms of a P -induced reduction of the involved scattering processes (not only as an enhancement of $N(E_F)$ as in Fig. 3); this suggests that (i) within the metallic state ($T > T_L$), the electron-phonon or electron-electron interactions are reduced and that (ii) for $T < T_L$, P induces a partial (but weak) delocalization of those carriers that had been previously localized.

From above it is concluded that $\text{Fe}_{1+\delta}\text{S}$ is intrinsically metallic but below T_L localization effects are manifested. Then it is interesting to investigate the influence of localization on the electronic states at the Fermi surface. We addressed this question by carrying out a PES study using UPS. Fig 4 shows a UPS spectra near E_F measured using a Xe I source of $h\nu = 8.44$ eV under ultrahigh vacuum at $T = 300$ K. We observed a broad spectra with no Fermi edge: a non-metallic state which should be contrasted with the metallic features observed in $\text{Fe}_{1+\delta}\text{Te}$.³⁸ The presence of localization in this system could account

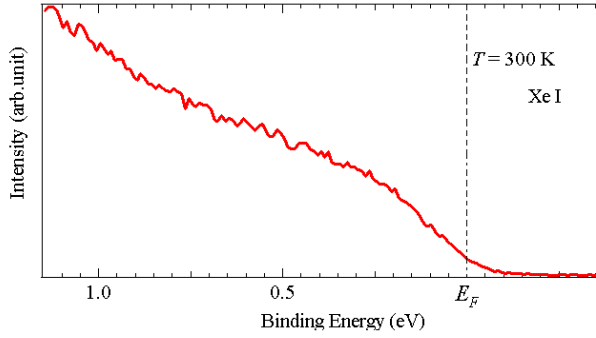


FIG. 4. UPS spectrum of $\text{Fe}_{1.08}\text{S}$ near E_F (dashed vertical line) using a Xe I source ($h\nu = 8.44$ eV), under ultrahigh vacuum at $T=300$ K.

for these features. We observed the same phenomenon with the He I (21.2 eV) and He II (40.8 eV) spectra but given the greater mean free path of the Xe I source (ca. $1\mu\text{m}$) we take this result as being more representative of the bulk sample.

The phase instability of $\text{Fe}_{1+\delta}\text{S}$ can be best illustrated by $\rho(T, P)$ of Fig. 5: on a first cooling branch, $\rho(T, 3\text{GPa})$ shows metallic behavior followed by a localization-induced uprise below T_L . On warming, $\rho(T, 3\text{GPa})$ follows the cooling curve except at high- T wherein thermal lag is manifested due to thermal gradients that are generated across the massive body of the pressure cell. On a second cooling branch, after some days at room temperature, $\rho(T, 3\text{GPa})$ was found to be completely modified, showing an absence of metallic-like behavior and an uprise on lowering the temperature which starts already at 300K. This irreproducibility is related to the above mentioned phase instability: indeed post-measurement XRD data indicated a partial phase transformation to the hexagonal troilite form but with no evident change in the lattice parameters of the remaining mackinawite phase. Evidence of amorphous material (most probably amorphous mackinawite) was also found.

IV. DISCUSSION AND CONCLUSIONS

Fig. 2(a) is a manifestation of a pressure-induced enhancement of the stability of the metallic phase.³⁹ Similar enhancement had been observed in the $R\text{NiO}_3$ charge-transfer perovskites,³⁵ wherein a metal-insulator transition at T_{MIT} marks the sharp uprise in $\rho(T < T_{\text{MIT}})$ and, furthermore, the monotonic decrease in $T_{\text{MIT}}(P)$ is related to the P -induced decrease in the charge-transfer gap. In spite of the similarity in the manifestation of the localization and the associated P -induced effects, we believe that the crossover event in $\text{Fe}_{1+\delta}\text{S}$ is not due to an Anderson-type metal-insulator transition because (i) the is no low- T AF order or a strong hysteresis effects, (ii) the rise in $\rho(T < T_L)$ is weak ($\sim\text{m}\Omega\text{-cm}$), smooth and extends over a wider temperature range, and (iii) there are

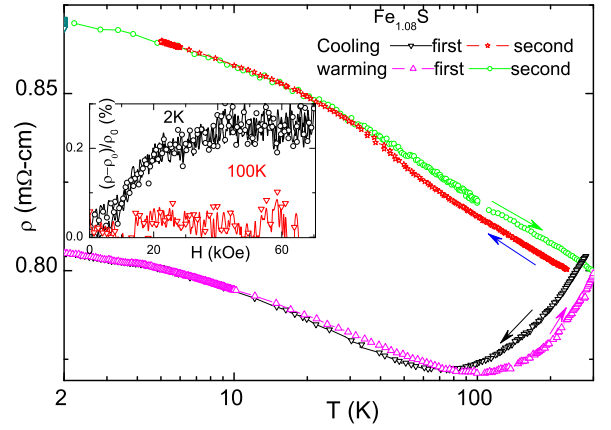


FIG. 5. Various resistivity curves of $\text{Fe}_{1.08}\text{S}$ measured under 3.0 GPa: the resistivity curve during the first cooling is similar to the first warming (taking into consideration the inherent thermal lag due to the massive body of the pressure cell). On a second cooling, the resistivity deviates strongly from the first cooling curve: this is related to phase instability. On a final warming branch, the resistivity retraces the behavior of the second cooling. The inset shows that the magnetoresistivity measured at 2 K (circles) and 100 K (triangle).

two (an activated and a log-in- T) processes operating at different temperature regions. Instead, it is assumed that there is a weak localization process which is due to scattering from any non-periodically arranged potentials (the most probable disorder/defects centres are the randomly distributed excess Fe or chalcogens deficiencies as in $\text{Fe}_{1+\delta}\text{Te}$ and $\text{Fe}_{1+\delta}\text{Se}$).^{4,33,36}

The manifestation of two types of localization processes is not unique to $\text{Fe}_{1+\delta}\text{S}$; it had been already observed in thin films³⁰ though the order of appearance, as T is varied, is inverted. The activated behavior (Eq. 1) within $100\text{ K} < T < T_L$ is taken to be due to a hopping of carriers. On the other hand, the log-in- T (Eq. 2) behavior below 20 K is attributed to quantum corrections arising from scattering from the above mentioned non-periodic potentials.³⁰

The log-in- T relation³⁰ is also valid for localization of weakly interacting carriers though with a different logarithmic prefactor.³¹ Alternatively, interaction effects in disordered 2D Fermi systems within the metallic regime can also give rise to a log-in- T relation.³² As is the usual practice, a distinction between whether a log-in- T behavior is due to either a non-interacting^{30,31} or an interacting carriers can be obtained from a magnetoresistivity experiment: on increasing H , a negative magnetoresistivity is manifested for the weak localization case while a positive one for the interaction case. The magnetoresistivity of $\text{Fe}_{1.08}\text{S}$ at 2 K (inset of Fig. 5) is positive indicating that interactions among the diffusing carriers are important.³² Such a manifestation of electron-electron interactions is taken to be behind the absence of superconductivity in $\text{Fe}_{1+\delta}\text{S}$: indeed no such strong field-dependent magnetoresistivity had been observed in the

isomorphous $\text{Fe}_{1+\delta}\text{Se}$ (see Fig.5 of Ref. 40). At higher temperature (>100 K), such a positive magnetoresistivity is drastically reduced while, at higher field, there is a tendency towards negative magnetoresistivity.

In summary, $\text{Fe}_{1+\delta}\text{S}$ is shown to be a metal but due to localization processes, such metallicity is not reflected in the thermal evolution of $\rho(T < 300\text{K})$ nor in the UPS spectra. Applied pressure does reduce the influence of the localization processes and as such the metallic character is manifested even for temperatures as low as 75 K at 3.0 GPa. Such a pressure influence is also evident in the Pauli-like susceptibility which is enhanced monotonically with P . Using low- T magnetoresistivity anal-

ysis, the weak localization that gives rise to a log-in- T behavior is suggested to be due to interaction effects in this disordered Fe-based system. It is assumed that such electron-electron interactions are behind the absence of superconductivity in this Fe-based chalcogenide.

ACKNOWLEDGMENTS

This work was supported in part by the Japan Society for the Promotion of Science (JSPS) and the Japan Science and Technology (JST) agency through the Strategic International Collaborative Research Program (SICORP-EU Japan).

-
- ¹ Y. Mizuguchi and Y. Takano, J. Phys. Soc. Jpn. **79**, 102001 (2010).
 - ² K. Deguchi, Y. Takano, and Y. Mizuguchi, Sci. Technol. Adv. Mater. **13**, 054303 (2012).
 - ³ A. Subedi, L. Zhang, D. Singh, and M. H. Du, Phys. Rev. B **78**, 134514 (2008).
 - ⁴ M. H. Fang, H. M. Pham, B. Qian, T. J. Liu, E. K. Vehstedt, Y. Liu, L. Spinu, and Z. Q. Mao, Phys. Rev. B **78**, 224503 (2008); T. J. Liu *et al.*, Nat. Mater. **9**, 716 (2010).
 - ⁵ C. Dong, H. Wang, Z. Li, J. Chen, H. Q. Yuan, and M. Fang, Phys. Rev. B **84**, 224506 (2011).
 - ⁶ Y. Kawasaki, K. Deguchi, S. Demura, T. Watanabe, H. Okazaki, T. Ozaki, T. Yamaguchi, H. Takeya, and Y. Takano, Solid State Commun. **152**, 1135 (2012).
 - ⁷ E. F. Bertaut, P. Burlet, and J. Chappert, Solid State Comm. **3**, 335 (1965).
 - ⁸ J. B. Goodenough, Mat. Res. Bull. **13**, 1305 (1978).
 - ⁹ J. A. Wilson, J. Phys.:Condens. Matter **22**, 203201 (2010).
 - ¹⁰ K. D. Kwon, K. Refson, S. Bone, R. Qiao, W. L. Yang, Z. Liu, and G. Sposito, Phys. Rev. B **83**, 064402 (2011).
 - ¹¹ A. Subedi, L. Zhang, D. J. Singh, and M. H. Du, Phys. Rev. B **78**, 134514 (2008).
 - ¹² A. J. Devy, R. Grau-Crespo, and N. H. Leeuw, J. Phys. Chem. C **112**, 10960 (2008).
 - ¹³ A. Kjekshus, D. G. Nicholas, and A. D. Mukherjee, Acta. Chem. Scand. **26**, 1105 (1972).
 - ¹⁴ L. Ehm and et al., J. Appl. Cryst. **42**, 15 (2009).
 - ¹⁵ J. L. Horwood, M. G. Townsend, and A. H. Webster, J. Solid State Chem. **17**, 35 (1976).
 - ¹⁶ J. R. Gosselin, M. G. Townsend, and R. J. Tremblay, Solid State Comm. **19**, 799 (1976).
 - ¹⁷ P. Waldner and A. D. Pelton, J. Phase Equilib. Diffus. **26**, 23 (2005).
 - ¹⁸ H. Kobayashi, T. Kamimura, Y. Ohishi, N. Takeshita, and N. Mri, Phys. Rev. B **71**, 014110 (2005).
 - ¹⁹ R. A. Berner, Science **137**, 669 (1962).
 - ²⁰ A. R. Lennie, S. A. T. Redfern, P. F. Schofield, and D. J. Vaughan, Mineral. Mag. **59**, 677 (1995).
 - ²¹ D. J. Vaughan and M. S. Ridout, J. Inorg. Chem. **33**, 741 (1971).
 - ²² D. Welz and M. Rosenberg, J. Phys. C: Solid State Phys. **20**, 3911 (1987).
 - ²³ S. Denholme, S. Demura, H. Okazaki, H. Hara, K. Deguchi, M. Fujioka, T. Ozaki, T. Yamaguchi, H. Takeya, and Y. Takano, Mater. Chem. Phys. (2014).
 - ²⁴ A. Rohrbach, J. Hafner, and G. Kresse, J. Phys.: Condens. Matter. **15**, 979 (2003).
 - ²⁵ H. Ikeda, M. Shirai, N. Suzuki, and K. Motizuki, Jpn. J. Appl. Phys. **32**, 301 (1993).
 - ²⁶ K. Shimada, T. Mizokawa, K. Mamiya, T. Saitoh, A. Fujimori, K. Ono, A. Kakizaki, T. Ishii, M. Shirai, and T. Kamimura, Phys. Rev. B **57**, 8845 (1998).
 - ²⁷ L. A. Taylor and L. W. Finger, Carnegie Institute of Washington Geophys. Lab. Ann. Rept. **69**, 318 (1970).
 - ²⁸ D. Cskbernyi-Malasics, J. D. Rodriguez-Blanco, V. K. Kis, A. Recnik, L. G. Benning, and M. Psfai, Chem. Geol. **294-295**, 249 (2012).
 - ²⁹ A. K. Stemshorn *et al.*, J. Mater. Res. **25**, 396 (2010); High Pressure Res. **29**, 267 (2009).
 - ³⁰ P. W. Anderson, E. Abrahams, and T. V. Ramakrishnan, Phys. Rev. Lett. **43**, 718 (1979); G. J. Dolan and D. D. Osheroff, **43**, 721 (1979).
 - ³¹ H. Fukuyama, J. Phys. Soc. Jpn. **48**, 2169 (1980); H. Fukuyama, Y. Isawa, and H. Yasuhara, **52**, 16 (1983).
 - ³² B. L. Altshuler and A. G. Aronov, Solid State Commun **46**, 429 (1983).
 - ³³ M. ElMassalami *et al.*, J. Phys.: Conf. Ser. (proc. 27th Intern. Conf. on Low Temperature Physics (LT27), Buenos Aires ,Argentina) (2014).
 - ³⁴ N. F. Mott, Rev. Mod. Phys. **40**, 677 (1968); J Physics C: Solid State Physics **20**, 3075 (1987).
 - ³⁵ X. Obradors *et al.*, Phys. Rev. B **47**, 12353 (1993); X. Granados *et al.*, **48**, 11666 (1993).
 - ³⁶ T. J. Liu *et al.*, Phys. Rev. B **80**, 174509 (2009); H. H. Chang, J. Y. Luo, C. T. Wu, F. C. Hsu, T. W. Huang, P. M. Wu, M. K. Wu, and M. J. Wang, Supercond. Sci. Technol. **25**, 035004 (2012).
 - ³⁷ I. T. Sines, D. D. V. II, R. Misra, E. J. Popczun, and R. E. Schaak, J. Solid State Chem. **196**, 17 (2012).
 - ³⁸ Y. Xia, D. Qian, L. Wray, D. Hsieh, G. F. Chen, J. L. Luo, N. L. Wang, and M. Z. Hasan, Phys. Rev. Lett. **103**, 037002 (2009).
 - ³⁹ H. Okada, H. Takahashi, Y. Mizuguchi, Y. Takano, and H. Takahashi, J. Phys. Soc. Jpn. **78**, 083709 (2009).
 - ⁴⁰ Y. Mizuguchi, F. Tomioka, S. Tsuda, T. Yamaguchi, and Y. Takano, Appl. Phys. Lett. **93**, 152505 (2008).